Antimisting Action of Polymeric Additives in Jet Fuels

Polymeric solutes in jet fuel can serve to increase greatly the droplet size and reduce flammability in fuel sprays created by high-velocity wind shear. Photographic and spark-ignition studies show that high molecular weight polyisobutylenes can be effective at levels below 100 ppm, where they cause only slight increases in fuel viscosity. The effectiveness of the polymers increases with molecular weight and is very well correlated by the elongational viscosity of the solution, as measured by the ductless siphon height.

K. K. CHAO, C. A. CHILD, E. A. GRENS II, and M. C. WILLIAMS

Chemical Engineering Department
University of California, Berkeley
Berkeley, CA 94720

SCOPE

The addition of polymeric solutes at low concentrations to jet fuels is known to suppress ignition of the fuels under circumstances often encountered in aircraft crash landings (Weatherford and Wright, 1975). The additives, which are termed "antimisting" (AM), alter the morphology of the fuel sprays produced from ruptured fuel tanks and prevent the formation of fine fuel mists. Thus, the use of such AM agents in jet fuels has the potential to save the many lives that are lost in post-crash aircraft fires. However, the mechanisms by which these additives function are not well characterized, and the influence of the nature of the additive and the properties of the fuel/additive solution on the AM action remains to be explained. The objectives of this study were to relate the morphological and ignition characteristics of sprays of jet fuel containing selected AM additives to the rheological properties of the fuel solutions and, in turn, to the nature and concentration of the additive used. Previous studies, which often attempted to provide a full-scale representation of aircraft crash conditions (e.g., Ahlers, 1977), have not established such fundamental relationships under well-characterized conditions.

In this work, AM behavior was examined for eight polymeric additives (six of them polyisobutylenes) in Jet-A fuel (essentially a kerosene), for seven of them in toluene, and for several other additives in water, all over the concentration range of 50 to 3,000 ppm. Sprays were created by wind-shear action across the end of a vertical fuel-supply tube at controlled air velocities and fuel rates. The resulting sprays were recorded photographically for characterization of their droplet sizes and shapes. Flammability of the jet fuel sprays was determined for electric spark ignition at energies up to about 0.5 J. Physical properties of the additive/solvent solutions were also measured, including the surface tension, shear viscosity, drag reduction effect, and "ductless siphon" height, the latter a measure of elongational viscosity (Bird, et al., 1977). The molecular weight distributions of the polyisobutylenes were determined by gel-permeation chromatography.

CONCLUSIONS AND SIGNIFICANCE

The results of the mist-formation experiments conducted here indicated that all of these AM agents work by similar mechanisms, regardless of the chemical nature of the additive or the solvent, and under all spray conditions. Examination of photographs of the sprays showed that increasing additive concentrations led first to suppression of smaller droplets and formation of larger ones, then to distortion of droplet shapes to multiple filaments, and, ultimately, to the degeneration of the spray to one, or a very few, large filaments. This behavior was almost identical for all systems and spray conditions, with only the concentration at which the AM effects occurred changing from case to case. Very small concentrations of some AM agents generated significant visible changes in mist formation, with less than 100 ppm sometimes being able to eliminate small droplets and cause filaments to form. The most effective polymeric additives were those with the highest molecular weight.

The measurement of fuel mist flammability was an even more sensitive indicator of AM action than were the spray photographs, with total suppression of ignition by 0.55 J sparks being achieved at additive concentrations where droplet size increase was barely discernible in photographs. Ignition suppression under these conditions could be obtained with only 10 ppm of the most effective polyisobutylene additive. The ranking of the additives as to AM effectiveness according to ignition results was the same as that from photographic studies, with polymer molecular weight, M, being the primary indicator of effectiveness.

Although the degree of AM action, and of flammability reduction, was not correlated with solution viscosity and only slightly related to drag-reduction effects, it was found to be strongly correlated with the maximum ductless siphon height, h^*, supported by the solution. Since this height is a measure of the elongational viscosity, $\bar{\eta}$, of the solution, we can conclude that elongational viscosity plays a primary role in the AM action of these solutions. This also seems plausible in view of the stretching action involved in droplet deformation and filament breakup. High stretching rates can magnify $\bar{\eta}$ by several orders of magnitude, and such rates are found in high-velocity dispersive actions. Moreover, the extreme sensitivity of $\bar{\eta}$ to M is consistent with the same trends in AM phenomena. A rough criterion for polyisobutylenes appears to be that only molecules with $M > 10^7$ are truly effective, so that molecular-weight distribution data on the polymer are useful in determining its potential utility.

The conditions of spray formation, that is the air velocity and fuel/air ratio in the spray, also influenced the spray morphology and flammability for cases where AM additives were used. Flammability of the sprays generally increased with air velocity over the range of 40 to 90 m/s and with fuel-to-air mass ratios up to about 6. These observations are consistent with several reports of behavior of fuel sprays without additives (Mizutani and Nishimoto, 1972) and represent the effects of increased dispersion at higher velocities and greater droplet concentration at larger fuel loadings.

From this investigation it appears that effective antimisting

and flammability reduction for jet fuel can be achieved at very low concentrations (<100 ppm) of suitable polymeric additives, and that the effectiveness of the additives can be evaluated on the basis of their ability to increase $\overline{\eta}$ of the fuel/additive solutions. The most effective agents examined here, high-molecular-weight polyisobutylenes (such as Oppanol B230 from BASF), are able to achieve their AM actions at far lower concentrations than required for the additives most often studied in earlier work (e.g., AM-1, FM-9). The AM effects can be achieved with only very slight increases in the viscosity of the solutions, and thus viscous-flow demands for fuel pumping are not significantly greater than with pure fuel. Other pumpability problems can arise, and there may be increased pressure needed for flow through fuel filters, due to fluid elastic effects (Mannheimer, 1979).

The degradation of the polymers in these solutions by shear action, both incidental to normal handling and deliberately as a preliminary to fuel-filter passage and combustion of the fuels in jet engines, is an important phenomenon that remains to be carefully examined. This question, together with pump performance and filter flow problems, must be addressed before application of AM agents to jet fuels for civil aviation.

INTRODUCTION

The use of polymeric solutes to reduce the dispersion, and thus the flammability, of jet fuel in aircraft crashes has been investigated since the late 1960s; early studies were reviewed by Weatherford and Wright (1975). These, and later studies (Ahlers, 1977; San Miguel, 1978; Wright and Stavinoba, 1973; Zinn et al., 1976), involved full- or large-scale tests of aircraft crashes, fuel loss from aircraft wings, or impacts of projectiles on fuel tanks. They employed only a few proprietary AM additives (AM-1 from Continental Oil Co.; FM-4 and FM-9 from ICI, Ltd; XD-8132 from Dow Chemical Co.) at relatively high concentrations of from 1,000 to 7,000 ppm (by weight). Even experiments that created and studied sprays and their ignition under better controlled conditions (Polymeropoulus and Sernas, 1976) were restricted to these proprietary additives and high concentrations. Thus, although these investigations established that polymeric solutes could be effective under suitable conditions in reducing mist formation and fuel flammability, they were not able to relate the antimisting phenomena to physical properties of the fuel/additive solutions nor to the fundamental characteristics of the polymeric solutes. Such relationships are necessary for an understanding of AM action of the solutes and for development of AM agents that will be effective at much lower concentrations and with fewer undesirable effects (e.g., fuel viscosity increase, dissolution difficulties).

Although the mechanisms by which the polymeric additives function are far from clear, superficially one can attribute the reduced mist flammability to the fact that droplets in sprays of AM fuels tend to be larger than normal and, in some cases, deformed to strings or filaments (Eklund and Cox, 1978; Zinn et al., 1976). The dominant effect would seem to be the reduction of surface area available for vaporization, combined with a greater distance between droplets to inhibit flame propagation. However, work with fine mists of pure fuel suggests that other factors may be important where very small droplets ($< 10\ \mu m$) are present (Burgoyne and Cohen, 1954; Burgoyne, 1957). Most work with sprays produced by wind shear, or by atomizing nozzles, indicates that flame velocities (and flammability) decrease with increasing drop diameters (Mizutani and Nishimoto, 1972; Polymeropoulos and Das, 1975). Polymeropoulos and Sernas (1976) found similar behavior for Jet-A fuel containing the commercial additives AM-1, FM-4, and XD-8132 at concentrations of 0.2 to 0.7%. San Miguel (1978) also reported the same general effect of droplet size in AM fuel sprays created in an apparatus simulating large-scale discharge from an airfoil.

Relationships between the physical properties of fuel/additive solutions and AM performance have received relatively little attention. Zinn et al. (1976) observed the breakup (under wind-shear action) and flammability of sprays of Jet-A fuel and solutions containing 0.2% AM-1, 0.4% FM-4, and 0.7% XD-8132 in a 1.53-m (5-ft) diameter wind tunnel; all tests were made at a wind speed of 57 m/s (110 knot) and at fuel flows of 30 to 53 g/s (4 to 7 lb/min). They also measured shear viscosities for the solutions, but established no consistent relationship between viscosity and AM effectiveness. The only correlation available between fuel rheological properties and AM behavior has been that reported by Hoyt et al. (1980), who examined the breakup of liquid discharge jets (3.2-mm exit diameter, 310-kPa upstream pressure) for a number of polymeric additives in Jet-A fuel at concentrations from 100 to 2,000 ppm. The enhanced stability of such jets can be interpreted in terms of fluid viscoelasticity, as explained by Goren and Gottlieb (1981) who invoked a nonlinear continuum mechanics model for their analysis. Hoyt et al. also measured turbulent drag reduction in a capillary for these solutions and found that the ranking of additives by effectiveness as drag-reduction agents (minimum concentration for maximum drag-reduction effect) corresponded generally to their observed effectiveness as AM agents, judged from photographs of the sprays. Furthermore, this ranking showed good correlation with the molecular weight of the agent, where M was known. The work of Hoyt et al. served to demonstrate the potential for use of appropriate solution properties as measures of expected AM activity; it did not yield a quantitative measure (beyond ranking) of effectiveness of polymeric additives nor address the question of flammability reduction, which may occur in the absence of visible changes in spray structure. Sarohia (1981) has recently discussed possible relationships of elongational viscosity and drag reduction to the performance of fuels with AM agents, but he did not evaluate additives on this basis and presented no quantitative correlations.

The investigation described here was thus directed to the question of which rheological properties of fuel/additive solutions best correlate with both visible AM action and measured flammability reduction, with emphasis on the degree to which the molecular weights of members of a largely homologous series of polymeric additives characterize their AM capability. To this end the sprays of solvent/additive solution created by wind-shear action were classified as to structure from high-speed photographs and were tested for flammability when subjected to sparks of calibrated energies up to 0.55 J. Rheological properties of the solutions, including shear viscosity η and elongational viscosity $\overline{\eta}$ (indirectly), as well as drag reduction performance, were measured and examined for correlation with their AM behavior. None of the additives produced any significant change in the surface tension of Jet A fuel at the concentrations investigated here.

EXPERIMENTAL

Spray Apparatus

Studies of spray morphology and flammability were conducted in a relatively small-scale apparatus in which sprays are created by wind-shear action of an air jet passing horizontally over the end of a vertical tube through which fuel is supplied at a controlled rate. This apparatus, Figure 1, consists of an atomizer for formation of the spray, a secondary air supply for variation of air-to-fuel ratios, and an observation chamber for photographic and flammability studies of the sprays.

In the atomizer, fuel is supplied to a vertical, 1.0-mm ID tube by a calibrated syringe pump. Primary air from a 1.75-mm ID nozzle is directed horizontally across the end of the fuel supply tube as shown in Figure 1;

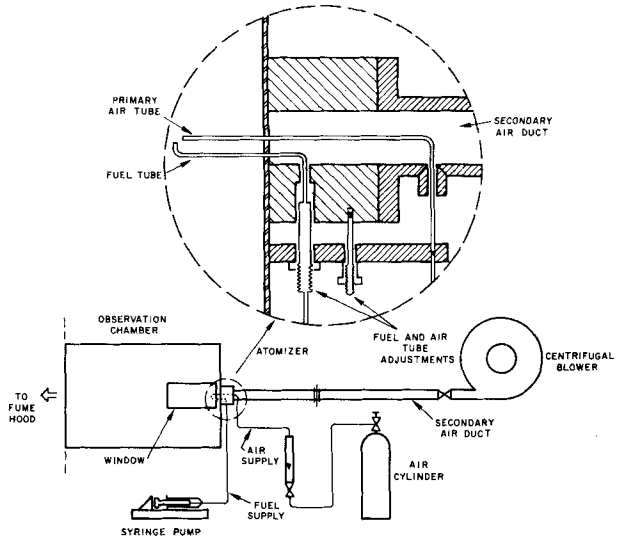

Figure 1. Spray creation apparatus.

this primary air is supplied from a compressed gas cylinder through a regulator, a rotameter, and needle valve for control of its flow. The atomizer is positioned concentric to, and 45 mm downstream from, the end of a 25-mm ID secondary air supply duct that is fed by a centrifugal blower, whose air flow is controlled with a butterfly valve and measured with an orifice meter.

Spray from the atomizer is directed into the 380-mm square by 660-mm long observation chamber, which discharges at its downstream end into a laboratory fume hood and is otherwise enclosed, except for the centrally located 25 mm entry for the atomizer/secondary air duct on the upstream end. This chamber is fitted on both sides with 64 × 200 mm quartz windows for spray observation and photography, and with electrode holders for a spark ignition device.

The apparatus is capable of spraying fuel at rates of 0.06 to 1.3 cm^3/s with primary air velocities of 20 to 90 m/s (45 to 201 mph). Air-to-fuel mass ratios of 0.1 to 10 can be obtained. A more complete description of the device, and associated equipment and procedures, is given by Child (1981).

The sprays were photographed in the observation chamber with a 35-mm camera (Nikon FM) equipped with a 105-mm Micro-Nikkor lens arranged to give an image/object ratio of 1:1. The film used was Kodak Plus-X. To obtain photographs of the rapidly moving droplets, a high-speed (10 μs), high-intensity (1.8×10^6 lumen) stroboscopic light source was employed (General Radio Strobolume 1532-D). It was located at the window opposite the camera to give back-illumination, with a single sheet of sub-20 ($75\ g/m^2$) bond paper placed in front of the light source as a diffuser.

Flammability was tested by electrical spark discharge between tungsten alloy electrodes spaced 5 mm apart and placed horizontally across the spray at its centerline and 55 mm downstream from the atomizer. Sparks were produced by an electronically-triggered capacitor discharge device, operating at 15 kV, and able to produce sparks of 0.1 to 0.55 J at repetition rates up to $2\ s^{-1}$. The spark energies for this device were controlled by capacitor switching and were calibrated from simultaneous oscilloscope traces of spark voltage and current.

The procedure used in photographic and flammability studies consisted of loading the fuel supply system with previously prepared solutions, establishing required air flows, and then initiating fuel flow at the desired rate. For photographic studies three exposures were taken with the prefocused camera before flow conditions were changed. For flammability studies, spark energies were increased at about 30 s intervals (using $1\ s^{-1}$ repetition rate) until ignition was observed or the maximum spark energy was reached; this procedure was repeated at least three times. In some cases flammability was tested only at maximum spark energy (0.55 J), sprays being classified as flammable if any ignition was observed in about 30 s. Sparks of this magnitude are large enough to yield results realistic in the context of aircraft landings.

Rheological Apparatus

Solvent and solution shear viscosities, η, were measured in conventional gravity-flow capillary viscometers of the Ostwald type. Density and inertial corrections (Van Wazer, 1970) to the data in these tests were negligible,

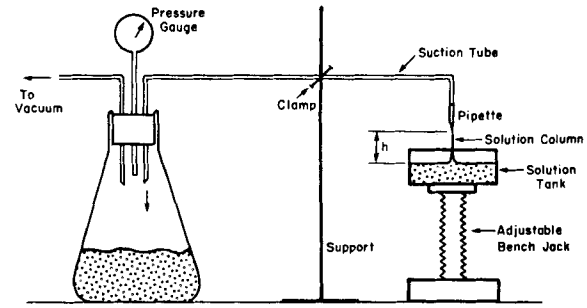

Figure 2. Ductless siphon.

and no evidence of non-Newtonian effects could be seen under the shearing conditions of these viscometers.

In view of the correlational success of Hoyt et al. (1980) with turbulent drag reduction, a simple capillary flow system was also established here for drag reduction studies. A heavy-walled glass Erlenmeyer pressure flask of 4-L volume was the liquid reservoir, with pressure up to about 10^5 Pa (15 psig) provided from a compressed air cylinder and measured by a gauge inserted through the flask stopper. Liquid flowed from the flask through a 3.8-mm ID Tru-Bore glass capillary, also inserted through the stopper, into another flask for collection of a measured mass (converted to volume using the known density) during a given time, so that volumetric flow rate was easily obtained. Tests with different capillary lengths showed that end effects were unimportant; a length of 0.916 m was used for most tests. Design parameters permitted easy access to the Reynolds Number range $500 < Re < 5 \times 10^4$, and drag reduction was evident within this range for almost all the solutions tested. Details of the measurements are described by Chao (1981).

The major novelty in rheological characterization in this work was adoption of the "ductless siphon" as a measure of elongational viscosity, $\bar{\eta}$. This siphon phenomenon, long a mere curiosity, is the rise of an unsupported liquid column from a quiescent pool into the opening of a capillary, suspended above the pool and providing suction to draw the column upward. The height of the column, h, can be impressive; values as large as 24 cm were achieved in these studies.

The basic explanation of this siphon effect lies with fluid elasticity and, in view of the importance of stretching motions in such a flow, with $\bar{\eta}$ as the controlling parameter. Thus, the flow continues because elongational strain rates are high enough in the rising column to generate sufficient tensile stress to support the column weight. If the pool is lowered, h grows but column weight now provides a greater load and slows the flow; eventually, strain rate is reduced to the point where rheological stresses can no longer support the column and the column breaks (its height at this point is designated h^*). Surface tension plays no significant role. Normal stress coefficients defined for shear flows are irrelevent to an extensional flow such as this; if any event, these are extremely small in dilute solutions and were not measurable with available equipment.

For correlation purposes, we can take h^* as a measure of $\bar{\eta}$. An approximate analysis (Chao, 1981) suggests that h^* is proportional to $(\bar{\eta}/\eta)^{1/2}$. While the siphon flow is far from a uniform elongational flow field (Peng and Landel, 1976), there is currently no device available for true $\bar{\eta}$ measurement in dilute solutions, and the ductless siphon is a simple, effective and inexpensive tool. Values of h^* can be reproduced to about ±5% with some operator experience.

The siphon device used is displayed in Figure 2. The inside tube diameter was 5.0 mm narrowed to 1.0 mm at the inlet to enhance local strain rates. A tube length of 1.1 m and a suction of about 4×10^4 Pa (300 mm Hg) were used. Measurements were initiated by immersion of the tip in the pool and establishment of a flow under the standard suction. (Results for h^* were insensitive to the suction chosen.) The pool was then slowly lowered as a bench jack supporting it was turned down. Values of h, measured against a vertical scale, were observed carefully as the column thinned and finally separated at h^*.

Materials and Properties

The AM effects on spray morphology, and the corresponding rheology, were studied for solutions in Jet-A, toluene, and water; Jet-A solutions were also tested for flammability. Jet-A fuel, from Shell Oil Co., had a density of $0.80\ g/cm^3$ and a vapor pressure of about 5,000 Pa at 293 K. Care was taken to keep the fuel and its solutions enclosed until testing to prevent variable loss of volatile components. The toluene was reagent grade and the water single-distilled; densities were 0.866 and 0.998 g/cm, respectively,

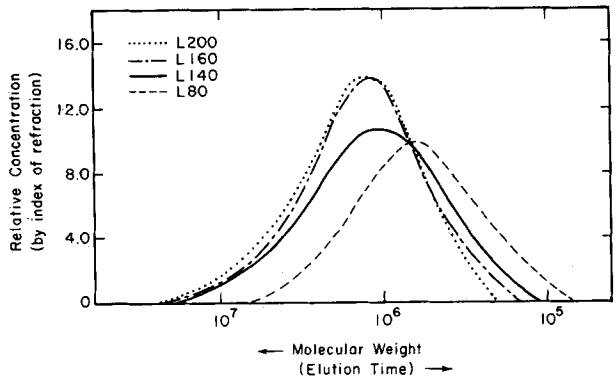

Figure 3. Molecular weight distributions by GPC for the Vistanex series of polyisobutylenes.

at 293 K. Solvent viscosities at 293 K were: 1.78, 0.59 and 1.00 mPa·s (cp) for Jet A, toluene and water, respectively.

The polymers examined as AM agents were: six polyisobutylenes (PIB), a Vistanex series with four "L" grades (from Exxon Chemical) and an Oppanol series with two "B" grades (from BASF); one polyethylene oxide (PEO) in grade WSR-301 from Union Carbide; three polyacrylamides (PAM) as Separan grades from Dow Chemical; one styrene/butadiene/styrene triblock copolymer (Kraton 1101) from Shell Chemical; and a non-PIB proprietary additive that has been widely used in previous studies (here designated PX). Molecular weight distributions for the PIB additives were obtained by gel permeation chromatography (GPC) using a Waters Associates liquid chromatograph and four microStyragel columns with a toluene eluting solvent; distributions for the Vistanex samples are shown in Figure 3.

All polymers were characterized in terms of intrinsic viscosity $[\eta]$ in each solvent,

$$\lim_{c \to 0} \frac{\eta(c) - \eta_s}{c\eta_s} \equiv [\eta] \tag{1}$$

where η_s is solvent viscosity and c is polymer mass concentration. Because $[\eta]$ is a measure of polymer coil domain volume in a particular solvent, and thus reflects both polymer and solvent character (Ferry, 1970), it is an important parameter. Values of both $[\eta]$ and the corresponding viscosity-average molecular weight, $\overline{M}_v$, are shown for the systems studied here in Table 1. For the PIB samples, the number and weight-average molecular weights, $\overline{M}_n$ and $\overline{M}_w$, from the GPC curves are also displayed.

Drop-size distribution in liquid sprays can be affected also by the liquid/air surface tension. This has been described for specific types of apparatus (e.g., Janna and John, 1979, for fan-jet pressure nozzles) and is a general consequence of hydrodynamic stability even for the case of viscoelastic liquids (Goren and Gottlieb, 1982). Therefore, surface tensions of Jet-A solutions were measured with a Rosano Surface Tensionmeter.

TABLE 1. PROPERTIES OF ANTIMISTING AGENTS

Agent	mol. wt. × 10^{-6} $\overline{M}_n$	$\overline{M}_v$	$\overline{M}_w$	$[\eta]$, dL/g Jet-A	Toluene	Water
Polyisobutylene						
Vistanex						
L 80	0.65	0.68	1.75	—	1.6	—
L140	1.3	2.30	4.51	—	3.2	—
L160	1.4	4.11	5.04	5.8	4.4	—
L200	1.1	5.00	5.37	7.8	4.9	—
Oppanol						
B200	1.4	5.70	6.02	8.5	5.3	—
B300	1.1	7.37	9.00	9.2	6.1	—
Polyethylene Oxide						
Polyox 301	—	2.50	—	—	—	7.8
Polyacrylamide						
Separan NP10	—	1.14	—	—	—	6.8
Separan AP30	—	2.64	—	—	—	12.0*
Separan AP 273	—	5.23	—	—	—	19.2*
PX	—	—	—	0.9	—	—
Kraton 1101†	0.08	—	—	—	—	—

* With 4% NaCl to suppress expansion of polyelectrolyte at low c.
† Styrene/butadiene/styrene copolymer, 30% styrene.

However, as might be expected, the values of surface tension for the solutions never deviated significantly (less than 2% increases) from the value found for Jet-A (0.0263 N/m at 293 K).

RESULTS AND DISCUSSION

The antimisting, ignition suppression, and rheological effects of the polymeric additives investigated here were determined at concentrations ranging from 5 to 3,000 ppm by weight. In all, 12 polymers and 19 polymer/solvent combinations were studied for AM action, and six PIB/Jet-A systems plus the PX/Jet-A system were examined in ignition tests; specific solvent/additive combinations studied are listed in Table 2. Studies of spray morphology and flammability were conducted at fuel rates of 0.06 to 1.3 cm^3/s and primary air velocities of 45 to 89 m/s, all at ambient temperatures of 291 to 297 K. These flow conditions represent wind-shear velocities of about 100 to 200 mph and fuel-to-air mass ratios of 1.5 to 6, representative of relatively severe conditions that might be encountered in aircraft crash landings.

Spray Morphology

The effect of AM additives on spray structure was evaluated from photographs of the sprays. These photographs, enlargements

TABLE 2. ANTIMISTING CLASSIFICATION OF SOLVENT/ADDITIVE SPRAYS: AIR VELOCITY, 67 m/s; FUEL FLOW 0.33 cm^3/s

Solvent	Additive	Concentration (ppm) 50	100	250	500	1,000	2,000	3,000
Jet A	L80	1	1	1.5	2	2.5	3	3
	L140	2	2	2.5	3	3.5	4	4
	L160	2	2	2.5	3	3.5	4	4
	L200	2	2.5	2.5	3.5	4	4.5	4.5
	B200	2	2.5	3	3.5	4	4.5	5
	B230	2.5	2.5	3	4	4.5	5	5
	Kraton 1101	—	—	—	—	—	—	1
	PX	1	1	1.5	2	3	3.5	4
Toluene	L80	1	1	1	1	1.5	2	—
	L140	1	1.5	2	2	2.5	3	3
	L160	1	1.5	2	2.5	3.5	3.5	—
	L200	1.5	1.5	2	2.5	3	4	4
	B200	1.5	1.5	2	2.5	3	4	4.5
	B230	1.5	1.5	2.5	3	4	4	4.5
	Kraton 1101	—	—	—	—	—	—	1
Water	Polyox	—	1.5	2.5	3.5	4	4.5	5
	NP10	—	1	1	1	2	2.5	3
	AP30	2	2.5	3	3.5	4	5	5
	AP273	3	4	5	5	5	5	5

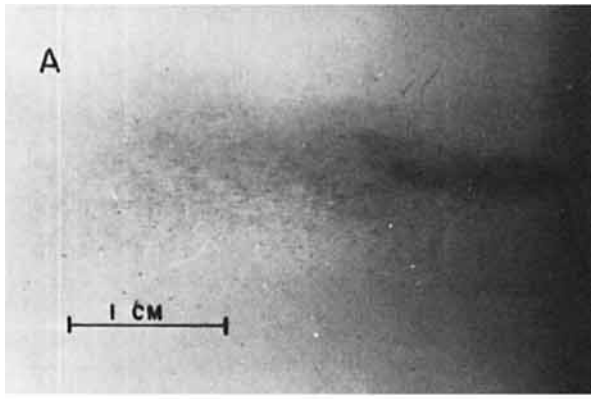

Frame A. Pure Jet-A fuel

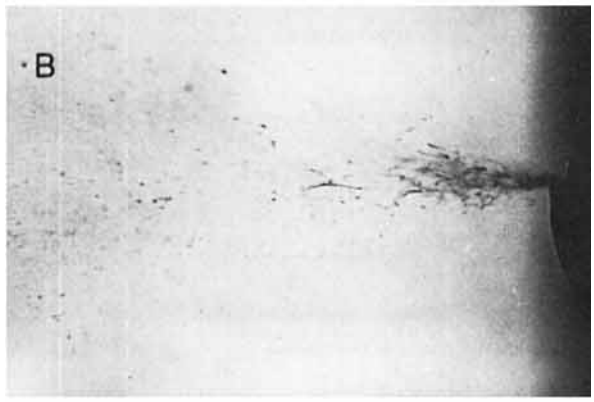

Frame B. B200 concentration = 50 ppm

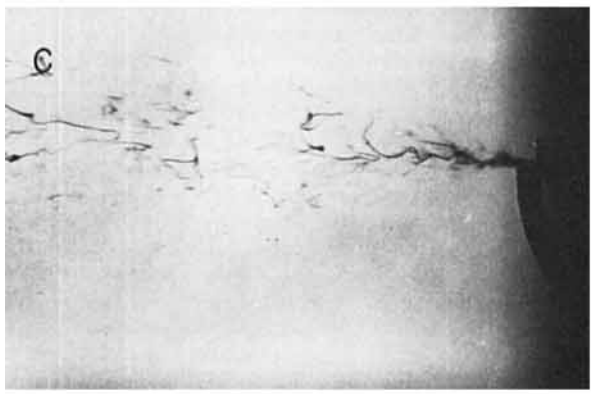

Frame C. B200 concentration = 250 ppm

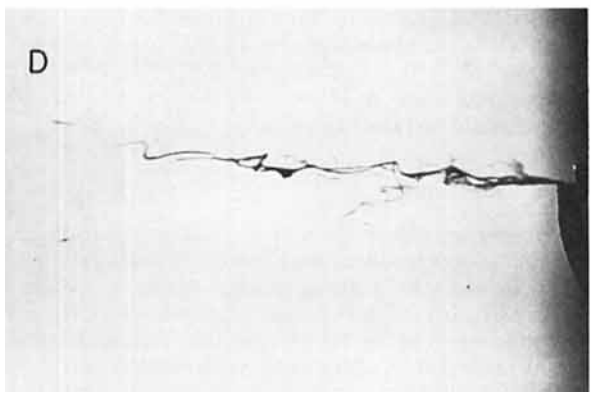

Frame D. B200 concentration = 1,000 ppm

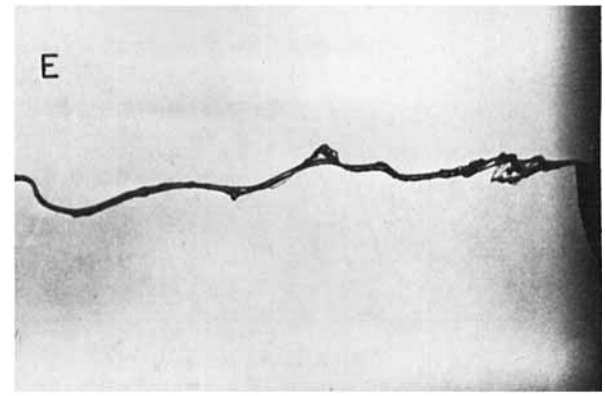

Frame E. B200 concentration = 3,000 ppm

Figure 4. Effect of AM additive concentration on spray morphology; Oppanol B200 in Jet-A at air velocity = 67 m/s, fuel flow = 0.33 cm³/s.

from 35-mm negatives, could resolve droplets to 20-μm diameter; thus effects on very fine particles could not be observed. For larger particles, the photographs demonstrated dramatic changes in the morphology of the sprays as the concentration of some of the additives was increased over the range of 50 to 3,000 ppm; this was observed for all spray conditions (fuel flow and air velocity). These effects did not depend on η levels; tests with pure glycerin and pure water gave the same apparent spray morphologies, even though their viscosities differed by a factor of order 1,000, whereas polymeric solutions exhibiting dramatic changes in their sprays possessed viscosities only slightly larger than those of pure solvents (about 1–5 mPa·s).

These changes can be seen in Figure 4, which shows the effects of Oppanol B200 on Jet-A sprays at a fuel flow of 0.33 cm^3/s with 67 m/s air velocity. Frame A shows a pure Jet-A spray composed only of small, spherical droplets, most smaller than 50 μm (the greater part of the spray is in droplets too small for photographic resolution). The addition of 50 ppm of B200, as in Frame B, changes the structure of the spray by increasing droplet sizes and causing elongation of many droplets. An increase in AM agent concentration to 250 ppm leads to the formation of many convoluted filaments of fuel, together with relatively large deformed droplets, as seen in Frame C. Further increase in additive concentration to 1,000 ppm results in near elimination of droplets, the spray being comprised of multiple, twisted filaments (Frame D). Finally, at 3,000 ppm of B200, the Jet-A spray consists of only a single liquid filament illustrated in Frame E. This single filament persists for distances in excess of 1 m downstream of the atomizer without any breakup, similar to fluid behavior reported by Hoyt et al. (1980) for capillary jets.

Examination of the photographs for other additive/solvent combinations, and at other spray conditions, revealed that the same AM action was taking place in all cases, with the only difference being the additive concentration at which the effects appeared. Increases in fuel flow, at constant air velocity, had almost no effect on additive concentrations required for a given AM effect, while increases in primary air velocity slightly increased concentrations required for a given degree of mist suppression.

The similarity in AM behavior for all solvents, additives, and conditions led to a uniform classification system for the sprays that allowed semiquantitative evaluation of AM performance. The sprays were classified into categories 1 to 5, ranging from complete atomizaton to large filaments without breakup. These categories, defined below, are represented by Frames A through E of Figure 4.

- *Category 1:* Complete atomization, almost all droplets less than 50 μm (Frame A)
- *Category 2:* Initial presence of small filaments, many larger droplets (Frame B)
- *Category 3:* Mainly multiple filaments, but large droplets present (Frame C)

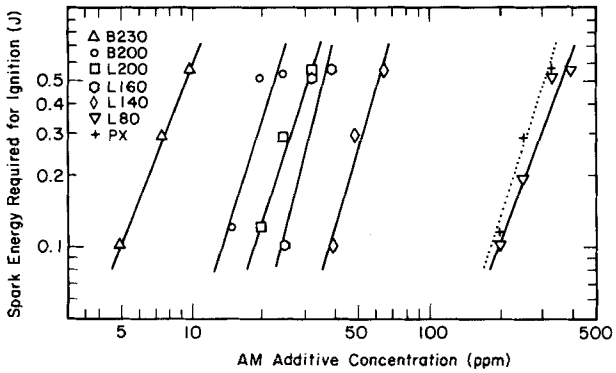

Figure 5. Effect of AM additive concentration on spark energy required for ignition of Jet-A sprays; air velocity = 51 m/s, fuel flow = 0.33 cm³/s.

- *Category 4:* Almost entirely several thin continuous filaments with very few droplets (Frame D)
- *Category 5:* One or two continuous large filaments with no liquid breakup (Frame E)

Although the category was assigned by judgment, it correlated extremely well with particle surface/volume ratios obtained from image analysis (Chao, 1981). With this antimisting classification (AMC) system, the effectiveness of the different additives can be measured and compared. This is shown in Table 2 for the systems studied here, evaluated at a fuel flow of 0.33 cm^3/s and an air velocity of 67 m/s. Results at other spray conditions are not much different. Comparison of the AMC for the various additives, and particularly for the homologous PIB polymers, with their average molecular weights given in Table 1, indicates that they rank in effectiveness, in any given solvent, exactly in order of their molecular weights, as suggested by Hoyt et al. (1980). Solvent has an effect, too, with the good-solvent cases yielding better AM performance than the poor-solvent cases (e.g., for PIB, Jet-A is a good solvent and toluene a poor one, as reflected by the relative magnitudes of $[\eta]$ in Table 1 for these systems).

Spray Flammability

Spark-ignition studies were conducted for six PIB additives and PX in Jet-A. The concentrations of additives required to prevent ignition were measured for spark energies from 0.1 to 0.55 J, with a fuel flow of 0.33 cm^3/s and an air velocity of 51 m/s (fuel-to-air mass ratio 1.8). These required concentrations increased only moderately with increasing spark energy, but differed markedly among the different PIB solutes, Figure 5. Rankings of the additives for their effectiveness in flammability reduction, and the magnitudes of differences in performance among additives, are exactly the same as was found for antimisting performance (Table 2). This strongly supports the conclusion that spray morphology alterations provide the mechanistic explanation for the ignition suppression behavior. However, in most cases, complete ignition suppression was accomplished at AM agent concentrations much lower than those required to yield a visible change in spray structure in the photographs, that is for the sprays still classified as category 1. This result can be traced to the importance of very small droplets (< 10 μm) in the flammability of sprays (Polymeropoulos and Das, 1975). Thus, the appearance of any filaments in sprays of AM fuels is a strong indication of effective flammability reduction for the circumstances in question, at least for fuels of high flash points (low vapor pressure) such as Jet-A. Furthermore, it allows spark ignition suppression to be used as a sensitive measure of the onset of AM activity in general.

The spark ignition results reported here, obtained with a small-scale apparatus, are in qualitative agreement with those obtained by Kapelke (1981) using a larger-scale flame-ignition device of the type described by Eklund and Neese (1978). Kapelke found a ranking of AM agents that was precisely the same as that

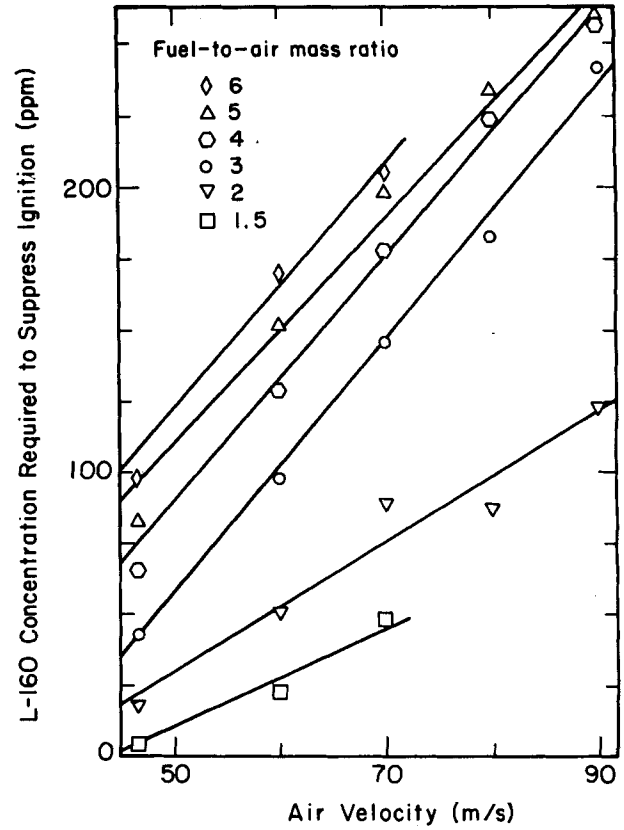

Figure 6. Effect of air velocity on flammability of sprays of Jet-A fuel containing L160 additive at several fuel-to-air ratios. Flammability measured as L160 concentration required to prevent ignition by 0.55-J spark.

determined here: B230 was the most effective, followed in order by B200, L160, PX, and other proprietary additives. Because of differences in test conditions and the presence of considerable quantities of undispersed liquid fuel near the ignition source, the additive concentrations Kapelke found necessary for ignition suppression were higher than those measured in this work.

The influences of air velocity and fuel-to-air ratio on flammability of AM sprays were investigated by measurement of the additive concentration required to suppress ignition by a 0.55 J (maximum) spark for different spray conditions. For most of this study the AM agent Vistanex L160 was used, because the low concentrations required for more effective additives reduced the sensitivity of the results. The relationship between air velocity and required concentration, for several air-to-fuel ratios, is shown in Figure 6 where the region below and to the right of each curve represents flammable conditions for the fuel/air ratio in question. As expected from results with pure fuels and from the photographic AM results, the flammability increases significantly with primary air velocity (because of increased fuel dispersion). Figure 6 also shows a marked increase in flammability with fuel-to-air ratio, an effect with no analogue observed in the photographic studies. This behavior is simply the result of increased particle number density in the sprays at higher fuel flows, rather than any changes in gross spray structure that would be noted in the photographs.

Molecular Parameters

The increasing AM effectiveness of additives with concentration c, M, and solvent/additive compatibility is nicely correlated by $[\eta]$ and the concept of polymer domain volume in solution. That is, if the polymer is effective in some proportionality to the volume fraction occupied by its coil, $[\eta]$ should be a useful lumped parameter. [Note that $[\eta]$ can be computed from KM^a (Ferry, 1970), where values of K and a can be obtained for many polymer/solvent systems (Brandrup and Immergut, 1975). This was used, here, to

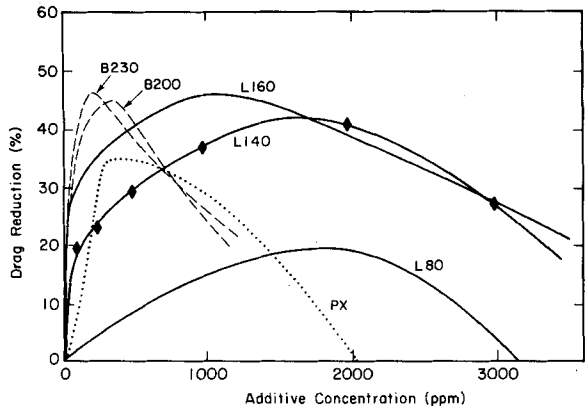

Figure 7. Drag reduction effect for polyisobutylenes and PX, at *Re* = 25,000 and 293 K. The PIB solutes are in toluene and PX is in Jet-A; both solvents are mediocre for the respective additives. To preserve clarity, data points are shown for only one curve.

obtain the $\overline{M}_v$ (given in Table 1) from measured $[\eta]$ values.] Even for higher c, the product $[\eta]c$ should be useful because all rheological properties can be represented as function of this variable alone up to $[\eta]c \simeq 1 - 2$, when domains begin to overlap extensively and entanglements may form. Up to that point, AM action would be considered primarily a single-molecule (i.e., dilute-solution) effect, as is also the case for drag reduction, which is effective at similar concentrations (Hoyt et al., 1980). One can compute an overlap concentration, c_o, at which coil domains begin to interact and thus signal departures from dilute behavior: $c_o \simeq 1/[\eta]$. Values of c_o (see $[\eta]$ in Table 1) are vastly greater than concentrations at onset of ignition suppression and even at onset of visible AM behavior. However, this individual-chain argument is weakened by the great coil elongations possible in elongational flows. It seems possible that stronger interpolymer interaction could be important when chains uncoil, since linear extensions of such huge molecules could bridge the distances between their centers of mass even in the nominally dilute solutions considered here.

Another aspect of molecular-weight effects is the distribution. It is likely that the extreme high tail of the distribution is disproportionately effective, and that averages such as $\overline{M}_v$ are not sufficiently reliable measures. For example, in Figure 2 three of the PIB additives have significant fractions with $M > 10^7$ while L80 has no fraction even approaching 10^7. Despite the $\overline{M}_v$ values being rather close (Table 1), the AMC rating for L80 falls far short of the others (Table 2) at all concentrations and with two solvents. Thus, molecular-weight distribution information can provide further insight about a candidate polymer's suitability for AM service.

Rheological Parameters

Drag Reduction. For flow through a capillary, a plot of pressure drop ΔP vs. flow rate for a given polymer solute at different concentrations (and $Re > 2{,}100$) gives a family of curves that shows clearly how ΔP first decreases with concentration (true drag reduction) and then increases, ultimately exceeding the curve for pure solvent (ΔP_s) because of increasing η. This effect is displayed in Figure 7 as the drag reduction ratio $(\Delta P_s - \Delta P)/\Delta P_s$ for PIB in toluene at the arbitrarily chosen $Re = 25{,}000$. While the drag reduction effect at low concentration correlates reasonably well with AM effectiveness for a given solution, as Hoyt et al. (1980) suggested, the decrease in drag reduction at higher concentration destroys the correlation. For example, if c is chosen arbitrarily for the comparison of two additives of different $\overline{M}$, their relative drag reduction effects may be totally meaningless; one could be on the increasing and the other on the decreasing portion of their respective drag reduction curves. On the other hand, AM action seems to be monotonic with concentration.

The major virtue of drag reduction as a predictor of AM effectiveness is that it is sensitive to extremely small polymer concentrations, where other rheological measurements (e.g., ductless siphon) may not show any effects. This is, for example, the case for L80 and PX. The greater sensitivity presumably stems from the higher local strain rates that can be present in turbulent flow than can be achieved in other apparatus. Thus, the low-c effectiveness of PX as a drag reducer in Jet A correlates well with its anti-ignition performance in Figure 5.

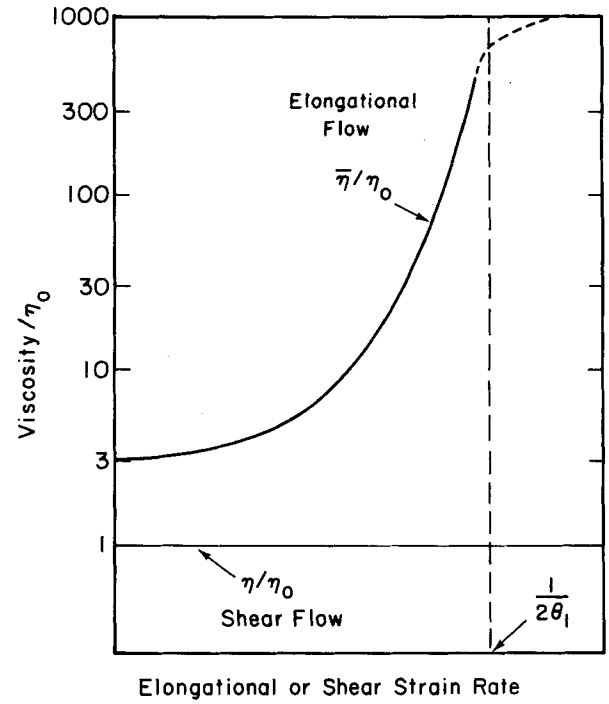

Figure 8. Expected behavior of elongational and shear viscosities as functions of strain rate, based on dilute-solution theories.

Ductless Siphon. The appearance of filaments in AM sprays (e.g., Figure 5) reflects the presence of a strong elongational mode in spray hydrodynamics. This, in turn, implies that $\overline{\eta}$ is a significant parameter, and could be the dominating one. This is plausible in view of the expected large magnitudes of $\overline{\eta}$ when solution elongational strain rate is large enough to extend the coil appreciably; Figure 8 illustrates the qualitative behavior predicted by dilute-solution molecular theories (Williams, 1975). As argued before, the maximum ductless siphon height, h^*, can be taken as a measure of $\overline{\eta}$ for correlation purposes.

For a given polymer, solvent effects on h^* are demonstrated by Polyox 301 in water (good solvent) and in toluene (poor solvent). The expected superiority of the good-solvent system over the entire

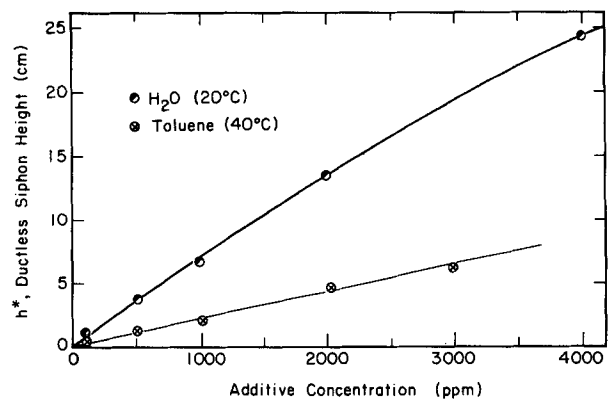

Figure 9. Effect of solvent on ductless siphon performance; Polyox 301 in water (a good solvent) and toluene (a poor solvent).

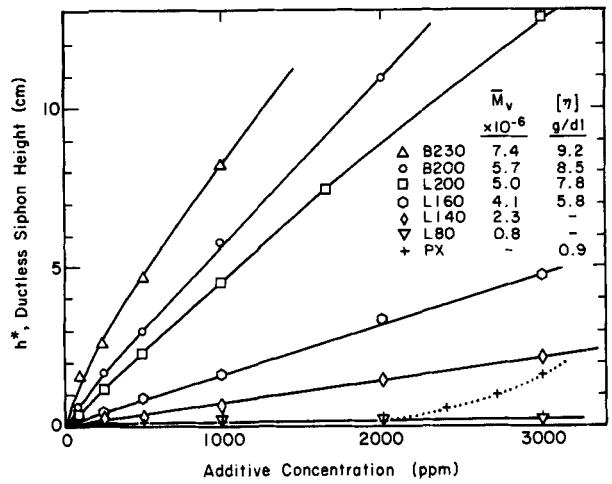

Figure 10. Effect of concentration on ductless siphon performance for PIB additives and PX in Jet-A.

concentration range is evident in Figure 9. Water is also a good solvent for the polyacrylamide additives, and h^* is correspondingly large for AP30 and AP273 (Chao, 1981). However, values of h^* for NP10 are comparable to those of water itself (up to $c \simeq 3{,}000$ ppm), presumably because NP10 contains a negligible fraction of material with $M > 10^7$ despite having $\overline{M}_v \simeq 1.1 \times 10^6$. Note that AMC values in Table 2 are correspondingly low for NP10 but high for AP30 and AP273.

The dependence of h^* on concentration for the PIB additives and PX in Jet-A is shown in Figure 10. The low h^* for L80 in Jet-A is due to the absence of any fraction with $M > 10^7$ (Figure 2) analogous to the case of NP10 in water. For PX, h^* starts to increase only at concentrations above 2,000 ppm; PX has been found to be an effective AM agent only at such higher concentrations. The relative positions of the curves for PIB additives correlate well with $\overline{M}$ but equally well with $[\eta]$. A distinction between these two measures of relative effectiveness can be made by examination of solvent effects, Figure 11; the three additives shown there produce

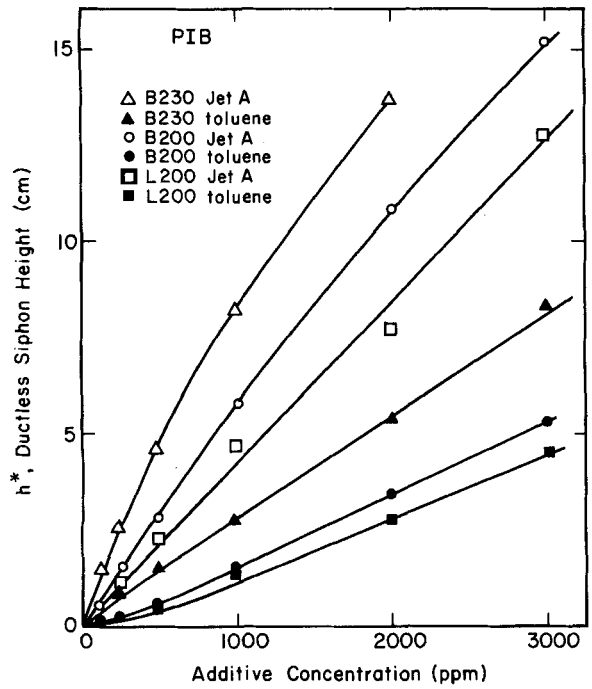

Figure 11. Effect of molecular weight and solvent compatibility on ductless siphon performance for PIB. Jet-A is a good solvent and toluene is a poor one.

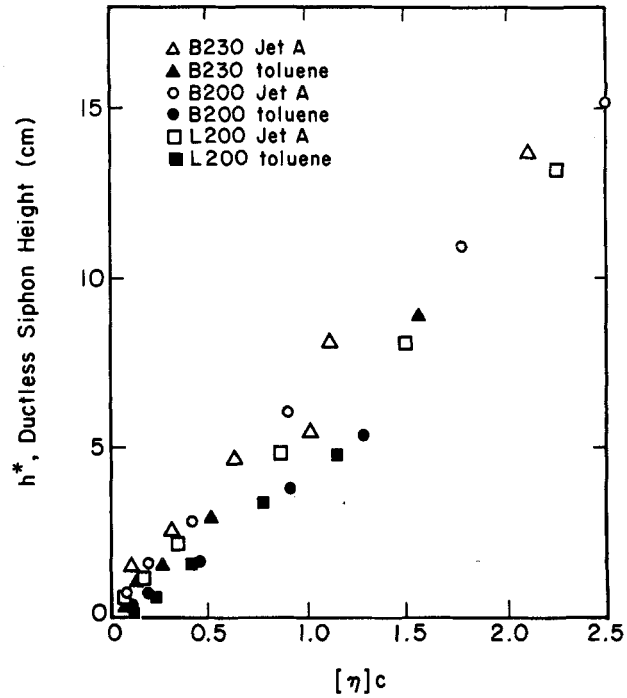

Figure 12. Dependence of ductless siphon performance on polymer-domain volume fraction in solution, as represented by [η]c.

very different h^* curves in Jet-A and in toluene. The sequence of curves is still ordered precisely according to $[\eta]$, but cannot be ranked by $\overline{M}_v$, verifying that h^* (and, thus, presumably $\overline{\eta}$), is predicted by $[\eta]$ as discussed earlier. If this is so, then dilute-solution molecular theories for $\overline{\eta}/\eta$ (Williams, 1975) can be invoked (Appendix A) to suggest that data on h^* can be correlated in terms of $[\eta]c$ as is done in Figure 12. There, even the minor differences between good-solvent data and poor-solvent data are in qualitative agreement with predictions of the theory (Appendix A). The rheological implications of these results are discussed in more detail by Chao (1981). In particular, it should be noted that $[\eta]c$ is so large that some of the measured values of h^* and the more spectacular changes in spray morphology are identified as *concentrated*-solution phenomena (i.e., $[\eta]c > 1$), although all significant trends are predicted correctly by dilute-solution theory.

From these arguments one might expect that h^* should be well correlated with AM performance. Indeed it is, as can be seen in Figure 13, where the AMC values for all polymer/solvent systems studied here are shown as a function of h^*. The importance of this result cannot be overstated: without any knowledge whatsoever

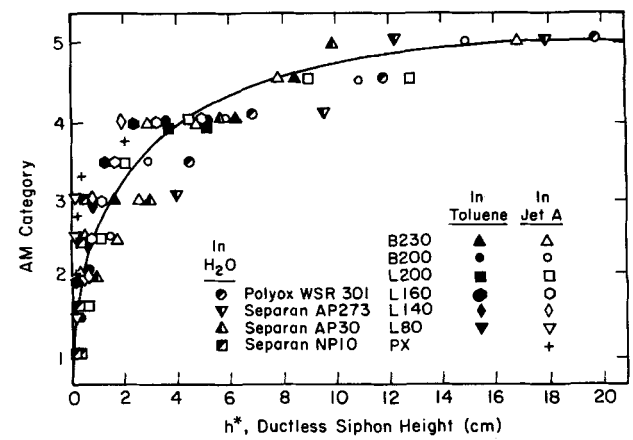

Figure 13. Correlation of AM category with ductless siphon performance for all additive/solvent combinations.

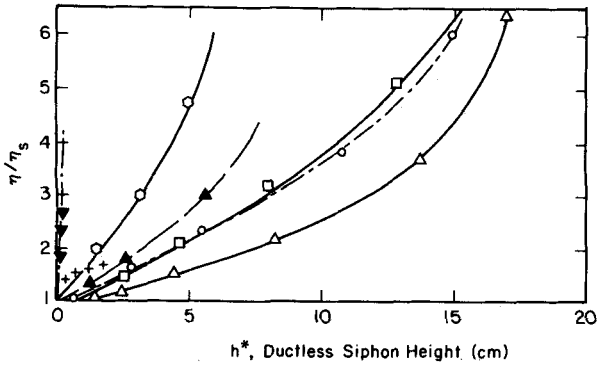

Figure 14. Relationship between viscosity increase and ductless siphon performance for PIB additives and PX in Jet-A. The lowest curve is most advantageous. Symbols are identified in Figure 13.

of the composition of a solution, or whether any degradation of the additive has occurred, one can forecast its AM performance by a simple measurement of ductless siphon height, h^*. This relationship should be of immense value in the laboratory screening of new AM agent candidates, and in the field testing for continued AM performance of modified fuels after preparation, handling, and storage.

Rheological Penalties. One of the concerns about use of polymeric additives in aircraft fuels is their enhancement of η, leading to increased pressure drops in fuel systems. While this is unavoidable, the penalty can be kept quite small if additive concentration is sufficiently low. However, there is a trade-off between requirements for high h^* (and $\overline{\eta}$) and for low η. Since the relationship between these parameters is unique for a given polymer/solvent combination, a set of η vs. h^* curves can be prepared for various additives and compared to find the polymer whose structure gives the most favorable behavior.

This is done in Figure 14 for seven of the polymer/solvent systems studied here. All curves are concave-up, indicating that the η penalty increases faster than the $\overline{\eta}$ benefit as both increase with additive concentration. Thus, truly dilute solution behavior does not prevail even at these low concentrations (or, possibly, h^* measurements contain artifacts not related to $\overline{\eta}$). The most effective system shown here, in the sense of this trade-off between η and h^*, is the polyisobutylene B230 in Jet-A. It is better by far than lower molecular-weight polyisobutylenes and the often-studied non-PIB additive PX. In general, the η vs. h^* curves are lower for higher polymer M and better polymer/solvent compatibility. The important implication for aircraft applications is that additives should be sought with the highest possible molecular weight, among those for which Jet-A is an extremely good solvent. The class of polyisobutylenes fulfills these criteria and has the potential for being less expensive than most other AM candidates (intrinsically, and also because of the low concentration needed).

ACKNOWLEDGMENT

Funds for the support of this study have been allocated by the NASA-Ames Research Center, Moffett Field, California, under Interchange No. NCA2-0R050-905. The authors also appreciate the assistance of R. A. Altman of NASA-Ames, who motivated this investigation.

NOTATION

c = concentration of additive, ppm (by weight) or g/dL
c_o = $1/[\eta]$
h = height of liquid column in ductless siphon
h^* = maximum value of h, at which column separates
M = molecular weight
$\overline{M}_n$ = number-average molecular weight
$\overline{M}_v$ = viscosity-average molecular weight, defined through $[\eta]$
$\overline{M}_w$ = weight-average molecular weight
ΔP = pressure difference across capillary
Re = Reynolds number for capillary flow

Greek Letters

$\dot{\gamma}$ = shear rate in simple shear flow, s^{-1}
$\dot{\epsilon}$ = elongational rate in pure extensional flow, s^{-1}
η = shear viscosity
$\overline{\eta}$ = elongational viscosity
$[\eta]$ = intrinsic viscosity, defined in Eq. 1, dL/g
θ = relaxation time for polymer chain, s

Subscripts

p = index for mode of polymer chain response dynamics
s = property that refers to solvent

APPENDIX A

In the classical theory of dilute monodisperse polymers modeled as chains of frictional beads and elastic springs (Williams, 1975), the predictions for viscosities are

$$\eta(\dot{\gamma}) = \eta_s + \frac{cRT}{M}\sum_p \theta_p \tag{A1}$$

$$\overline{\eta}(\dot{\epsilon}) = 3\eta_s + 3\frac{cRT}{M}\sum_p \left\{\frac{\theta_p}{(1-2\dot{\epsilon}\theta_p)(1+\dot{\epsilon}\theta_p)}\right\} \tag{A2}$$

where θ_p is the relaxation time of the pth normal mode of chain response. Note that η is predicted to be independent of shear rate $\dot{\gamma}$ (only mildly unrealistic for very dilute systems) but $\overline{\eta}$ ($\dot{\epsilon}$) is predicted to increase strongly with elongational rate $\dot{\epsilon}$ as $\dot{\epsilon} \to 1/2\theta_1$ where θ_1 is the longest relaxation time. This behavior is represented in Figure 8. Physically, the great increase in $\overline{\eta}$ is caused by the simultaneous great extension of the polymer coil; the theory ultimately fails as the extended chain length is predicted to grow to infinity when $\dot{\epsilon} \to 1/2\theta_1$ (reflected also in Eq. A2).

Despite the latter weakness, the theory explains why high molecular weight polymers exhibit such dramatically large $\overline{\eta}$ (or h^*) relative to lower molecular weight polymers. Since

$$\theta_p = k_p[\eta]M\eta_s/RT \tag{A3}$$

where k_p is a pure number related to eigenvalues of the dynamics problem, θ_p is itself very sensitive to M. With $\theta_1 \propto [\eta]M \propto M^{1+a}$, the limiting case $\overline{\eta} \to \infty$ is approached at far lower $\dot{\epsilon}$ ($\to 1/2\theta_1$) for large chains.

Furthermore, for correlation of ductless siphon height h^* for different solutions—related to $\overline{\eta}/\eta$ as suggested by Chao (1981)—some guidance is provided by combination of Eqs. A1–A3:

$$\frac{\overline{\eta}}{\eta} = 3\left\{\frac{1 + c[\eta]\sum_p \left\{\dfrac{k_p}{(1-2\dot{\epsilon}[\eta]MF_p)(1+\dot{\epsilon}[\eta]MF_p)}\right\}}{1 + c[\eta]\sum_p k_p}\right\} \tag{A4}$$

where $F_p \equiv k_p\eta_s/RT$ can be regarded as a set of constants. Note that the effects of solvent compatibility, c, and M are lumped into the product $[\eta]c$ as a first approximation, encouraging the correlation presented in Figure 12. Superimposed on this, however, is a deviation arising from terms in $\dot{\epsilon}[\eta]MF_p$ that do not contain c. One aspect of this deviation is that, at a given value of $[\eta]c$, $\overline{\eta}/\eta$ will be larger when the polymer is dissolved in good solvents, since then $[\eta]$ is larger and the critical condition $\overline{\eta}/\eta \to \infty$ is approached more closely at a given $\dot{\epsilon}$. This prediction is supported by trends in the data of Figure 12.

LITERATURE CITED

Ahlers, R. H., "Full-Scale Aircraft Crash Tests of Modified Jet Fuel," Federal Aviation Administration Report FAA-RD-77-13, U.S. Department of Transportation (1977).

Bird, R. B., R. C. Armstrong, and O. Hassager, *Dynamics of Polymeric Liquids*, 1 and (with C. F. Curtiss) 2, John Wiley & Sons, Inc., New York (1977).

Brandrup, J., and E. H. Immergut, *Polymer Handbook*, 2d Ed., Wiley-Interscience, New York (1975).

Burgoyne, J. H., "Mist and Spray Explosions," *Chem. Eng. Prog.*, **53**, 121 (1957).

Burgoyne, J. H., and L. Cohen, "The Effect of Drop Size on Flame Propagation in Liquid Aerosols," Proc. Royal Soc., **A225**, 375 (1954).

Chao, K. K. K., "Correlation of Rheological Properties and Anti-Misting Performances of Dilute Polymer Solutions," M.S. Thesis, University of California, Berkeley (1981).

Child, C. A., "Suppression of Jet Fuel Flammability by Polymeric Additives," M.S. Thesis, University of California, Berkeley (1981).

Eklund, T. I., and J. C. Cox, "Flame Propagation Through Sprays of Anti-Misting Fuels," NAFEC Technical Letter Report, NA-78-66-LR (1978).

Eklund, T. I., and W. E. Neese, "Design of an Apparatus for Testing the Flammability of Fuel Sprays," U.S. Federal Aviation Administration Report, FAA-RD-78-54, U.S. Department of Transportation (1978).

Ferry, J. D., "Viscoelastic Properties of Polymers," 2nd Ed., John Wiley & Sons, New York (1970).

Goren, S. L., and M. Gottlieb, "Surface Tension Driven Breakup of Viscoelastic Liquid Threads," *J. Fluid Mech.*, **120**, 245 (1982).

Hoyt, J. W., J. J. Taylor, and R. L. Altman, "Drag Reduction—Jet Breakup Correlation with Kerosene-Based Additives," *J. Rheology*, **24**, 685 (1980).

Janna, W. S., and J. E. A. John, "Drop-Size Distributions of Newtonian Liquid Sprays Produced by Fan-Jet Pressure Nozzles," *J. Eng. Industry*, **101**, 171 (1979).

Kapelke, M. S., "The Anti-Flammability Effectiveness of Polymers in Jet Fuel," Final Report on Grant NCC 2-140, NASA-Ames Research Center, Moffett Field, CA (1981).

Mannheimer, R. J., "Restoring Essential Flow and Ignition Properties to Antimisting Kerosenes for Turbine Aircraft Operations," Federal Aviation Administration Report, FAA-RD-79-62, U.S. Department of Transportation (1979).

Mitzutani, Y., and T. Nishimoto, "Turbulent Flame Velocities in Pre-mixed Sprays," *Combustion Sci. & Tech.*, **6**, 1 (1972).

Peng, S. T. J., and R. F. Landel, "Preliminary Investigation of Elongational Flow of Dilute Polymer Solutions," *J. Applied Phys.*, **47**, 4255 (1976).

Polymeropoulos, C. E., and S. Das, "The Effect of Droplet Size on the Burning Velocity of Kerosene-Air Sprays," *Combustion & Flame*, **25**, 247 (1975).

Polymeropoulos, C. E., and V. Sernas, "Ignition and Propagation Rates for Flames in a Fuel Mist," Federal Aviation Administration Report, FAA-RD-76-31, U.S. Department of Transportation (1976).

San Miguel, A., "Antimisting Fuel Kinematics Related to Crach Landings," *J. Aircraft*, **15**, 137 (1978).

Sarohia, V., "Fundamental Studies of Antimisting Fuels," AIAA/SAE/ASME 17th Joint Propulsion Conf., Colorado Springs, CO (July, 1981).

Van Wazer, J. R., J. W. Lyons, K. Y. Kim, and R. E. Colwell, "Viscosity and Flow Measurements," Wiley-Interscience, New York (1963).

Weatherford, Jr., W. D., and B. R. Wright, "Status of Research on Antimist Aircraft Turbine Engine Fuels in the United States," AGARD/NATO 45th Meeting. Propulsion and Energetics Panel, London (April, 1975).

Williams, M. C., "Molecular Rheology of Polymer Solutions: Interpretation and Utility," *AIChE J.*, **21**, 1 (1975).

Wright, B. R., L. I. Stavinoba, and W. D. Weatherford, Jr., "A Technique for Evaluating Fuel Mist Flammability," U.S. Army Fuels and Lubricants Research Laboratory Interim Report AFLRL-25, Southwest Research Institute, San Antonio, TX (1973).

Zinn, Jr., S. V., T. I. Eklund, and W. E. Neese, "Photographic Investigation of Modified Fuel Breakup and Ignition," Federal Aviation Administration Report FAA-RD-76-109, U.S. Department of Transportatin (1976).

Manuscript received April 29, 1982; revision received December 21, and accepted January 6, 1983.

Mass Transfer and Pressure Drop in a Cocurrent Reciprocating Plate Extraction Column

A 5-cm-diameter reciprocating plate extraction column has been operated in cocurrent flow. The pressure drop for water flow, and the local and average mass transfer products for the system acetic acid/kerosene/aqueous sodium hydroxide have been measured. Under well-agitated conditions, the mass average transfer product is predictable by a model, which is also applicable to data reported earlier by Karr for a 2.54-cm-diameter column.

S. H. NOH and M. H. I. BAIRD

Chemical Engineering Department
McMaster University
Hamilton, Ontario, Canada

SCOPE

Countercurrent liquid-liquid extraction may be performed in many types of column, among which the reciprocating perforated plate column developed by Karr (1959) is well known. Recently it was suggested (Karr, 1979) that the performance of the Karr column in cocurrent flow should be investigated. Although cocurrent extraction provides only one equilibrium stage, the throughput is not limited by flooding as in the case of countercurrent flow. The lack of a flooding problem also permits the use of intense agitation with correspondingly high mass transfer rates, unless the excessive agitation leads to unduly slow settling of the phases.

The general objective of this study is to examine the characteristics of a 5-cm-diameter reciprocating plate extraction column in cocurrent flow. Because the flows through the column